P2.8 EXAMINATION OF THE AZIMUTHAL VARIATION OF LONGWAVE RADIANCE FROM CERES DATA

Arvind V. Gambheer, David R. Doelling
AS&M Inc., Hampton, VA

Patrick Minnis
NASA Langley Research Center, Hampton, VA

1. INTRODUCTION

A precise knowledge of radiation budget is essential for understanding Earth's climate and weather. Accurate measurements of fluxes at the top of the atmosphere (TOA) are critical for estimation of radiation budget. Generally, satellite TOA longwave (LW) radiances are converted into fluxes using limb-darkening models that account for the variation of radiance with viewing zenith angle (VZA). The most recent limb-darkening models are dependent on geo-type, cloud amount, phase and optical depth as well as precipitable water, lapse rate and surface emissivity (Loeb et al. 2002). Figure 1 shows a schematic diagram of a satellite radiance measurement during daylight. Logically, a measurement of infrared (IR) radiance from the satellite position should produce a lower value than one from, say, the solar position because the illuminated area should be warmer than the shadowed area. Using limited matched satellite imager data, Minnis and Khaiyer (2000) showed that shadowing effects cause azimuthal variations of IR brightness temperatures over land that will impact estimates of surface temperature T_s and, perhaps, the TOA LW flux. They concluded that local topography, either as landforms or vegetation can cause these azimuthal variations and that the patterns vary with solar zenith angle or time of day. They found a high correlation between bidirectional reflectance anisotropy and the angular variation of T_s that depends on terrain variability. The Minnis and Khaiyer (2000) study was limited to narrowband infrared measurements from pairs of angles for a given time of day and location. A complete characterization of the azimuthal variation of T_s and the LW radiance would require measurements over all times of day from all angles at a given location. This requirement is impractical. However, with the availability of data from the Clouds and the Earth's Radiant Energy System (CERES) instrument on the Tropical Rainfall Measuring Mission (***TRMM***) satellite, it is possible to develop statistics on the azimuthal variation of both infrared window (WN; 8 - 12 μm) and LW (5 - 100 μm) radiances for various surface and terrain types for all times of day over the tropics and subtropics. Additionally, the CERES products include cloud properties as well as radiation data so that the azimuthal dependence can be explored for both clear and cloudy scenes. This paper begins the process of characterizing the azimuthal variation of LW and WN radiances to improve estimates of LW flux and T_s.

****Corresponding author address***: Arvind Gambheer, AS&M, Inc., 1 Enterprise Pkwy, Hampton, VA 23666. email: a.v.gambheer @larc.nasa.gov.

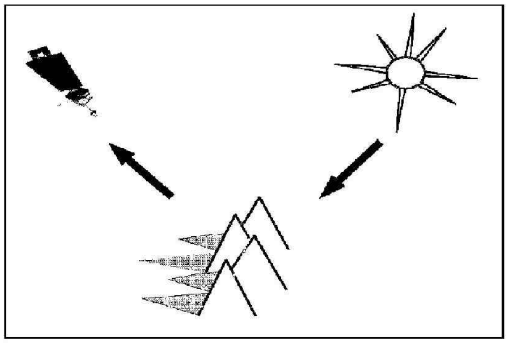

Fig. 1. Schematic of satellite-sun configuration with shadowing.

2. DATA

The CERES Single Scanner Footprint TOA/Surface and Clouds (SSF) data (Minnis et al. 2002) are used to examine the azimuthal variability. ***TRMM*** is in a 35° precessing orbit, limiting the coverage to about 37°S - 37°N. The SSF data include scanner data taken out up to VZA of 70°. During every third day, the CERES scanner operated in the Rotating Azimuthal Plane Scan (RAPS) mode. The RAPS data provide an unprecedented source of viewing a given region from multiple angles during a given overpass. The 68 days of available RAPS data taken from January through August 1998 are insufficient to derive regional models of radiance variability. Hence the CERES RAPS LW and WN radiances were averaged in angular bins as a function of time of day, surface type, topography, and cloud fraction. The relative azimuthal angle (RAA) span of 0 - 180° is divided equally into 9 bins of 20° and the VZA is binned at every 10° steps making 7 equal bins. The solar day is divided into 4 equal spans to accommodate the variability of solar zenith angle with latitude, namely 1) early morning, 2) late morning, 3) early afternoon and finally 4) late afternoon. Four cloud bins are defined based on cloud amounts: 1) clear (0-5%), 2) partly cloudy (5-50%), 3) mostly cloudy (50-95%) and 4) overcast (above 95%).

A total of 5 surface types, forests, shrublands, savannas, croplands and deserts, were defined by grouping the original International Geosphere Biosphere Program (IGBP) scene types. The 5'-resolution (~10 km) ETOP05 surface elevation data were used to define terrain variability. For each 5' region, the standard deviation of the surface elevation was computed for the region and the 8 adjacent regions to serve as a measure of terrain variability. The resulting value is

used to determine the index for grouping each region into one of four topographical bins for each surface type. The first topography bin (minimum) contains all regions having the lowest 60 percentile of surface variability and is labeled as minimum surface variability bin. The next bin, low-medium, uses the terrain variability percentiles between 60 and 80. The percentiles between 80 and 90 and between 90 and 100 define the next two bins, high-medium and maximum, respectively.

After averaging all data into the appropriate bins, the mean radiance is computed for each VZA bin by integrating over RAA. These averages, which characterize the limb darkening for each case, are used to calculate the equivalent Lambertian radiance L_e by integrating the VZA averages over all VZAs. The average WN radiances are converted to brightness temperature T. The relative limb-darkening was computed by subtracting L_e from each VZA bin average L_v. Figure 2, an example of relative limb darkening for clear savannas, shows that the mean radiances are sensitive to the time of day. More limb darkening consistently occurs during the early morning and early afternoon than during the late morning and late afternoon.

To isolate the azimuthal anisotropy ΔL_r, L_v is subtracted from the mean radiance L_r for each RAA bin in a given VZA bin. The resulting values are plotted following the convention shown in Fig. 3.

3. RESULTS and DISCUSSION

Figure 4 shows an example of ΔL_r for clear savanna during late morning and for maximum surface variability. Negative values predominantly occur in the left half of Fig. 4, the shadowed side. These results are consistent

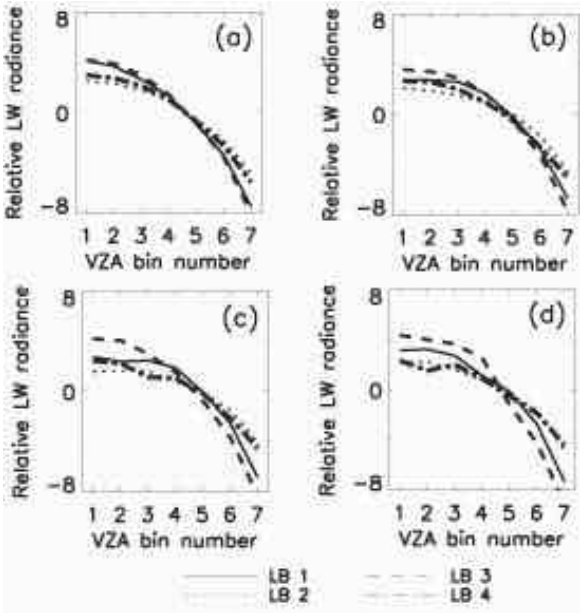

Fig. 2. TRMM relative LW radiances (in $Wm^{-2}sr^{-1}$) for savannas, for surface variability- (a) minimum, (b) low medium, (c) high medium and (d) maximum. LB refers to the local time bin.

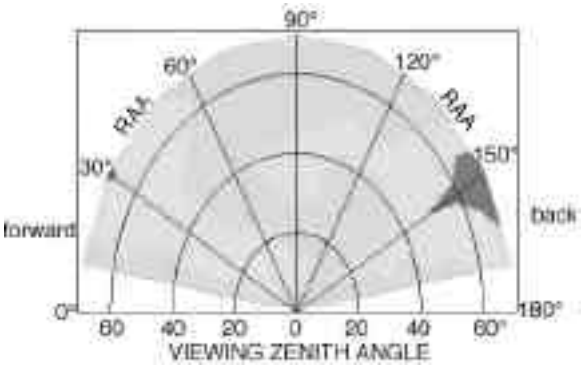

Fig. 3. Plotting convention for radiance and T anisotropy.

with expectations. The greatest positive values occur for VZA > 40° and for RAA > 150°. The solar "hot spot", the scattering angle unaffected by any shadowing, is close to VZA = 40° and RAA = 180° for this case. The minimum value occurs near VZA = 40°, RAA = 0°. Higher resolution binning could provide more detail of the anisotropy along the principal plane, but at the expense of reduced sampling. Differences as large as 8 $Wm^{-2}sr^{-1}$ are seen indicating that the anisotropy is very strong, even for average conditions. Greater or smaller differences will occur in a given instance. The maximum difference corresponds to a flux difference of about 24 Wm^{-2}.

Because there is minimal water vapor absorption in the WN band, the anisotropy should be stronger in the WN radiance field. The WN anisotropy is given as brightness temperature differences ΔT. Accordingly, L_v and L_r are first converted to temperature using the Planck function at 10 μm. Figure 5 shows ΔT during late morning for clear shrublands over the full range of terrain variability. The shadowed side is cooler than the sunlit side for all topographic conditions. The shading effects become more conspicuous as topographical variability changes from minimum to maximum. Temperature differences up to 10 K are observed between the sunlit and shaded sides. Unlike the results in Fig. 4, the minimum values occur between RAAs, 60° and 90°, at VZA > 40°. A secondary relative maximum appears at VZA > 60° in the forward scattering direction for all terrain types.

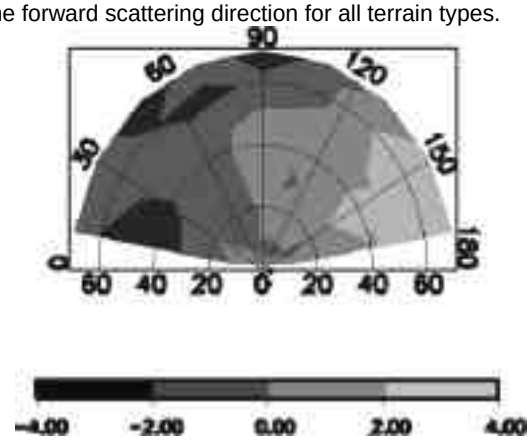

Fig. 4. TRMM LW anisotropy ΔL_r ($Wm^{-2}sr^{-1}$) for savannas. maximum surface variability, clear conditions, late morning.

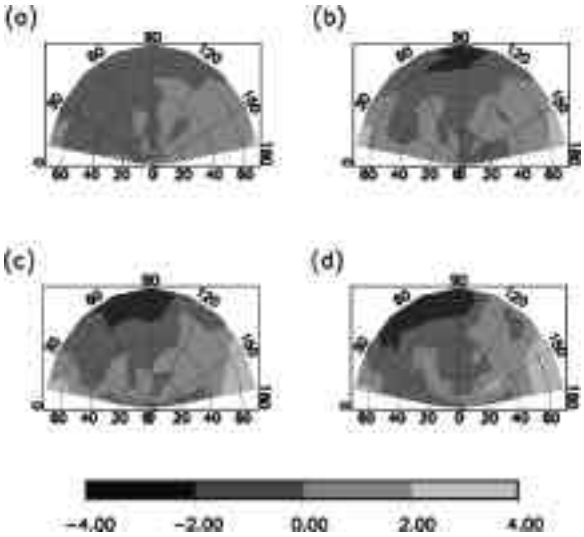

Fig. 5. TRMM WN anisotropy ΔT (K) for shrublands for clear conditions during late morning, for surface variability, (a) minimum, (b) low medium, (c) high medium and (d) maximum.

The WN anisotropy for the 4 local time bins is shown in Fig. 6 for clear savannas with maximum terrain variability. The minimum $\Delta \boldsymbol{T}$ in this case occurs closer to RAA = 0° for most times of the day. The anisotropy increases with time of the day until early afternoon and then starts decreasing. This type of variation occurs for all scene types with the largest positive values found between RAAs, 90° and 180°. Similar patterns are observed for other terrain conditions although the anisotropy is less pronounced. Similar analyses over ocean yield no distinct patterns with $\boldsymbol{L_r}$ varying by less than 1 Wm^{-2} sr^{-1}.

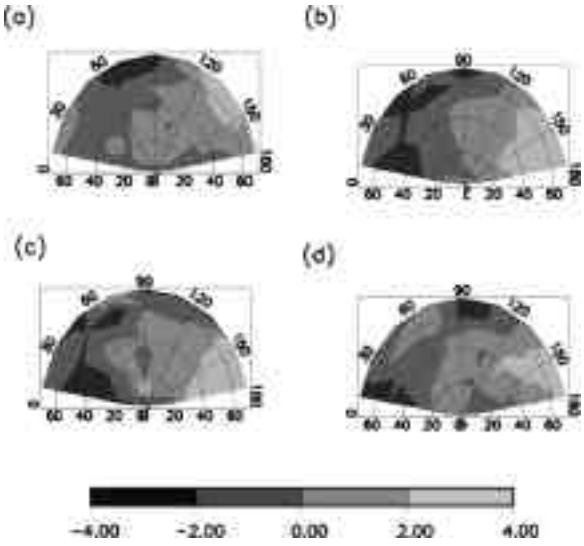

Fig. 6. WN temperature anisotropy in K for savannas in clear conditions with maximum surface variability (a) early morning, (b) late morning, (c) early afternoon and (d) late afternoon.

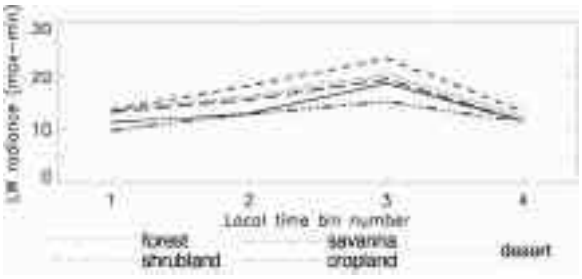

Fig. 7. TRMM LW bias (in $Wm^{-2}sr^{-1}$) as a function of local time.

The differences, $\Delta \boldsymbol{L_{mm}}$ or $\Delta \boldsymbol{T_{mm}}$, between the maximum and minimum radiance or temperature difference, respectively, provide a measure of the anisotropy for a given set of conditions and time of day. Figure 7 shows the temporal variation of $\Delta \boldsymbol{L_{mm}}$ for the 5 surface types with maximum terrain variability. The maximum differences occur over shrublands while the minimum is observed over forests. Maximum anisotropy occurs during the early afternoon. The observed LW radiances can be biased by as much as –16 to 8 $Wm^{-2}sr^{-1}$. Similarly, $\Delta \boldsymbol{T_{mm}}$, can be as large as 21 K, while the WN temperatures can be biased by –15 to 6 K. The results for less variable terrain are much like those in Fig. 7, except the magnitudes of the differences decrease with decreasing surface roughness.

The results presented so far are for clear conditions. Clouds also cause shadowing and should introduce some anisotropy in the emerging infrared radiation field. Figure 8 plots $\Delta \boldsymbol{T}$ for savannas under partly cloudy conditions during late morning. The forward viewing (shadowed) side is cooler than the back viewing (sunlit) side. The anisotropy is similar in magnitude to that seen for clear conditions. The values of $\Delta \boldsymbol{T_{mm}}$ decrease with increasing cloud cover, however, the basic pattern of positive values of $\Delta \boldsymbol{T}$ for RAA > 90° and negative values of $\Delta \boldsymbol{T}$ for RAA < 90° is still detectable over most surfaces during the late-morning and early afternoon periods, even for overcast conditions. Presumably, the azimuthal anisotropy would persist as long as a distinct shadow is evident underneath the cloud and would disappear when the solar illumination is entirely diffuse.

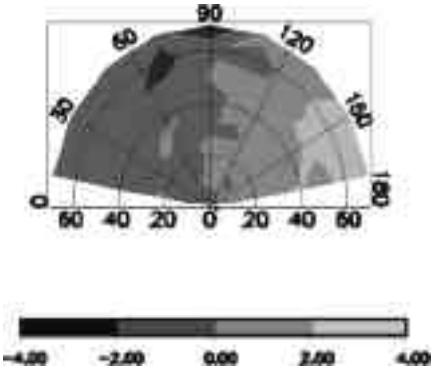

Fig. 8. TRMM WN temperature anisotropy in K for savannas for maximum surface variability and partly cloudy conditions during late morning.

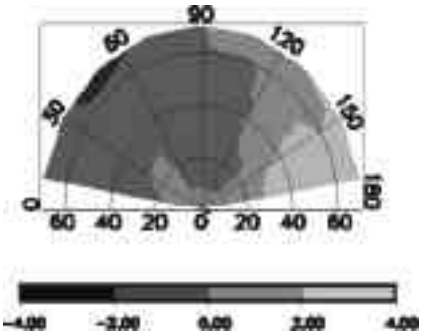

Fig. 9. Terra WN temperature anisotropy in K for savannas for maximum surface variability and partly cloudy conditions during late morning.

CERES is also operating on the ***Terra*** satellite, which is in a 1030-LT sun-synchronous orbit. It provides sampling over all latitudes but only for the late morning period. The ***Terra*** data for November and December 2000 were analyzed in the same manner as the ***TRMM*** data. Figure 9 shows ΔT for savannas with maximum surface variability during late morning derived from ***Terra***. The basic pattern in Fig. 9 is the same as that seen from the ***TRMM*** data. The similarity in patterns for the ***Terra*** and ***TRMM*** late morning period holds for all scene types, local time bins, and cloudy conditions but the anisotropy is consistently weaker than that from ***TRMM***.

The reduced signal from ***Terra*** might be due to differences in the areas that were sampled and to the orbital and scanning geometry. The TRMM results were limited latitudinally, while ***Terra*** samples all latitudes including the poles. An analysis of Terra data using only samples between 37°N and 37°S, however, produced essentially the same results found for latitudes between 50°N and 50°S. Thus, the orbit and scan angles may have a greater effect. Because the orbit is sun-synchronous during the morning, the CERES RAPS can only sample certain forward directions at later times while the anti-solar direction (backward) is sampled at earlier times. The ***Terra*** CERES swath is ~2330 km which corresponds to a time differential of 1.4 hr. Thus, the areas to the east have warmed under the sun for up to 1.4 hr longer than their western counterparts. Since the maximum ***T*** is expected in the western view and the minimum is expected in the eastern view when the local times are the same, the overall range should be reduced by the time differentials. The ***Terra*** CERES scan pattern is likely to have complicated effects on the derived anisotropy and should be studied further.

The ***TRMM*** CERES sampling pattern must also be carefully considered because the scan cannot sample certain angles near the top or bottom of the orbit, the latitude of 35°. A preliminary analysis of the data using only data taken between 30°S and 30°N yields more distinct anisotropic emission patterns and stronger anisotropy than observed here. Thus, it may be necessary to restrict the zonal coverage of CERES for computing the azimuthal effects.

4. CONCLUSIONS

Generally, more thermal radiation is observed on the sunlit side than on the shadowed side under most of the conditions. The observed range in equivalent temperature differences between the shadowed and sunlit sides for WN radiances are more than double those for LW radiances, most likely as a result of less atmospheric absorption in the WN region. The azimuthal signal is strong under clear conditions and the greatest RAA & VZA anisotropy occurs near noon**.** Azimuthal dependence of radiance appears to be a stronger function of topographical variability than vegetation type. RAA variation is greatest for shrublands and savannas and least for forests. Over deserts, it is less consistent than over other types possibly as a result of dramatic variability in surface albedo. The effects of such variability may not be entirely eliminated with the limited ***TRMM*** RAPS observational period. Azimuthal dependence was also seen for partly & mostly cloudy conditions and for some overcast cases. For oceans, the anisotropy signal is insignificant as expected. Angular anisotropy from ***Terra*** data is less than that from ***TRMM***, possibly because of orbital geometry differences between ***TRMM*** and ***Terra***.

Construction of correction models is underway and will take into account the sampling patterns of TRMM by restricting the latitudinal coverage of the data. Early afternoon data will soon become available from CERES on the recently launched ***Aqua*** satellite. If corrections for the swath time differential can be developed, then the sampling statistics for late morning and early afternoon can be greatly improved by combining results from CERES on ***TRMM***, ***Terra***, and ***Aqua***. Models developed from these datasets should be valuable for correcting LW observations from CERES, the Geostationary Earth Radiation Budget instrument on the Meteosat Second Generation satellite, Triana. Additionally, more accurate instantaneous estimates of surface skin temperature from IR imagers should be possible with these proposed corrections.

REFERENCES

Loeb, N. G., N. Manalo-Smith, S. Kato, W. F. Miller, S. Gupta, P. Minnis, and B. A. Wielicki, 2002: Angular distribution models for top-of-atmosphere radiative flux estimation from the Clouds and the Earth's Radiant Energy System instrument on the Tropical Rainfall Measuring Mission satellite. Part I: Methodology. Submitted ***J. Appl. Meteorol.***

Minnis, P. and M. M. Khaiyer, 2000: Anisotropy of land surface skin temperature derived from satellite data. ***J. Appl. Meteorol.***, **39,** 1117-1129.

Minnis, P., D. F. Young, B. A. Wielicki, D. P. Kratz, P. W. Heck, S. Sun-Mack, Q. Z. Trepte, Y. Chen, S. L. Gibson, R. R. Brown, 2002: Seasonal and diurnal variations of cloud properties derived for CERES from VIRS and MODIS data. ***Proc. 11th AMS Conf. Atmos. Rad.***, Ogden, UT, June 3-7.